한국해양공학회지 제14권 제1호, pp 11~16, 2000 (ISSN 1225-0767)

Computation of Two-Fluid Flows by Finite Volume Method and Discussion on Wave Breaking

SEUNG-HYUN KWAG* AND MILOVAN PERIC**
*Halla Univ., #66 Heungup, Wonju 220-712, Korea
**Tech. Univ. of Hamburg Lammersieth 90, D-22305 Hamburg, Germany

유한체적법에 의한 이층류 계산 및 쇄파에 관한 토의

곽승현* · Milovan Peric**
*한라대학교, **Tech. Univ. of Hamburg

KEY WORDS: Free surface 자유표면, Two fluid flows 이층류, Finite volume method 유한체적법, Submerged hydrofoil 수중날개, Interface capturing scheme 집면포착법

초 록: 수중날개를 대상으로 任意로 변형하는 二層流의 數値計算을 수행하였다. 計算은 非構造格子와 接面포착법을 이용하여 內山表面의 형상을 결정하였다. 本 硏究에 의하면 낮은 물속 깊이와 높은 프루드수에서 碎波현상이 발생하였다. 수중날개에 대하여 碎波형상의 效果를 연구하였고, 실험값과 계산값을 相互比較 함으로서 格子의 敏感性을 數値的으로 확인하였다.

1. Introduction

Numerical simulation of two-fluid flows, including the deformation of the free surface, is one of the big challenges in fluid mechanics. Many methods (Farmer *et al.*, 1994; Muzaferiza *et al*, 1997) of this kind have been developed and successfully applied to flows. However, if the body form is complicated, these methods are difficult to use because the grid has to be adapted both to the free surface and body shape: the grid may deform too much in this process and a re-gridding may become necessary. When the body form is relatively simple, the interface tracking approach is convenient in which only the water flow is computed and the grid moves to adapt to the free surface. Another difficulty in handling interface tracking methods is the breaking, overturning, or wave splashing. In many cases, it is important to compute the flows of both liquid and gas simultaneously, especially when the gas is enclosed by liquid and buoyancy effects become important. For this reason, interface capturing methods have to be used.

When a hydrofoil is close enough to the free surface and when its velocity exceeds a certain level, waves are generated at the free surface above it. They can be smooth or they may undergo breaking. The wave breaking causes fluctuations of both drag and lift; this can lead to vibrations on board of the vessel and may also cause structural damage. It is therefore of great practical importance to predict the flow around the submerged hydrofoils.

We present here computations of flows around submerged hydrofoils for two configurations: one that was studied experimentally by Duncan(1983) with non-breaking waves, to which both kinds of solution methods could be applied, and another with breaking waves, for which no experimental data is available and where only the interface-capturing approach can be employed.

2. Numerical Solution Method

The starting points are the mass and momentum conservation equations, which read in integral form:

$$\frac{d}{dt}\int_V \rho dV + \int_S \rho(\boldsymbol{v}-\boldsymbol{v}_b)\cdot \boldsymbol{n} dS = 0 \tag{1}$$

$$\frac{d}{dt}\int_V \rho u_i dV + \int_S \rho u_i(\boldsymbol{v}-\boldsymbol{v}_b)\cdot n dS = \int_S(\tau_{ij}-p i_j)\cdot n dS + \int_V \rho b_i dV \tag{2}$$

$$\frac{d}{dt}\int_V c dV + \int_S c(\boldsymbol{v}-\boldsymbol{v}_b)\cdot \boldsymbol{n} dS = 0 \tag{3}$$

where ρ is the fluid density, V is the control volume (CV) bounded by a closed surface S, $\boldsymbol{v}$ is the fluid velocity vector whose Cartesian components are u_i, $\mathbf{v}_b$ is the velocity of the control surface, t is the time, p is the pressure, b_i is the body force in the direction of the Cartesian coordinate x_i, $\boldsymbol{n}$ is the unit normal to S and directed outwards, and τ_{ij} are the components of the viscous stress tensor as,

$$\tau_{ij} = \mu\left(\frac{\partial u_i}{\partial x_j}+\frac{\partial u_j}{\partial x_i}\right) \tag{4}$$

with μ being the dynamic viscosity of the fluid. When the

control volume moves, the so called *space conservation law* (SCL) has also to be satisfied; it is expressed by the following relation between the rate of change of CV and its surface velocity:

$$\frac{d}{dt}\int_V dV - \int_S \boldsymbol{v}_b \cdot \boldsymbol{n} dS = 0 \tag{5}$$

For more details on discretization methods, see (Ubbink(1997), Muzaferiza *et al.*(1998)

Both fluids are treated as single effective fluids whose properties vary in space according to the volume fraction of each phase, i.e.,

$$\rho = \rho_1 c + \rho_2(1-c), \quad \mu = \mu_1 c + \mu_2(1-c) \tag{6}$$

where subscripts 1 and 2 denote the two fluids (liquid and gas). If one CV is partially filled with one and partially with the other fluid (i.e., $0 \le c \le 1$), it is assumed that both fluids have the same velocity and pressure.

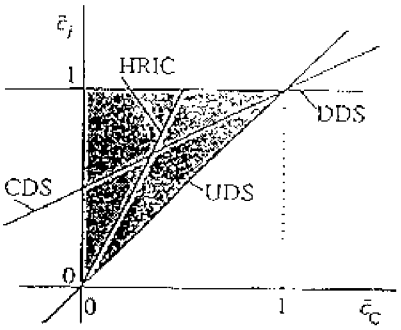

Fig. 1 Normalized variables diagram (CDS: Central Diff. Scheme, DDS: Downwar)

The sharpness of the interface without over- and undershoots can be achieved by limiting the approximation of the cell-face value to lie in the shaded area of the so called *normalized variable diagram (NVD)* (Leonard, 1997) shown in Fig. 1. The local normalized variable c in the vicinity of the cell-center C is defined

$$\tilde{c}(\boldsymbol{r}) = \frac{c(\boldsymbol{r}) - c_U}{c_D - c_U} \tag{7}$$

where subscripts '*U*' and '*D*' denote nodes upstream and downstream of the cell-center *C*, and *r* is the position vector. The particular choice selected here is indicated in Fig. 1 as HRIC (high resolution interface capturing).

$$C_o = \frac{\boldsymbol{v} \cdot \boldsymbol{n} S \Delta t}{\Delta V_c} \tag{8}$$

$$\tilde{c}_f = \begin{cases} \tilde{c}_C & \text{if} \quad \tilde{c}_C < 0.0 \\ 2\tilde{c}_C & \text{if} \quad 0.0 \le \tilde{c}_C \le 0.5 \\ 1 & \text{if} \quad 0.5 \le \tilde{c}_C \le 1.0 \\ \tilde{c}_C & \text{if} \quad 1.0 \le \tilde{c}_C \end{cases} \tag{9}$$

$$\tilde{c}^*_f = \begin{cases} \tilde{c}_f & \text{if} \quad c_o < 0.3 \\ \tilde{c}_C + (\tilde{c}_f - \tilde{c}_C)\dfrac{0.7 - C_o}{0.7 - 0.3} & \text{if} \quad 0.3 \le c_o \le 0.7 \\ \tilde{c}_C & \text{if} \quad 0.7 \le c_o \end{cases} \tag{10}$$

$$\tilde{c}^{**}_f = \tilde{c}^*_f \sqrt{\cos\theta} + \tilde{c}_C (1 - \sqrt{\cos\theta}) \tag{11}$$

Finally, the cell-face value of c is computed according to eq. (7) as

$$c_f = \tilde{c}^{**}_f (c_D - c_U) + c_U \tag{12}$$

3. Results and Computations

The computations are performed for two configurations with a NACA0012 hydrofoil under the free surface: one with non-breaking and another with breaking waves. The angles of attack are 5° and 30° , Froude number 0.567, Reynolds number 10^3 & 1.776 x 10^6, and turbulence model is of the k-ε RNG type. The number of cell is 13540, time increment is 0.0005 and the reference pressure is 10^5 Pa. The minimum value of y^+ is 5 and maximum 410.

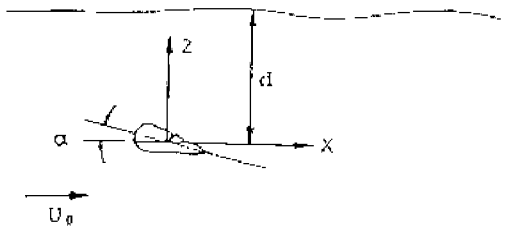

Fig. 2 Coordinate system for computation

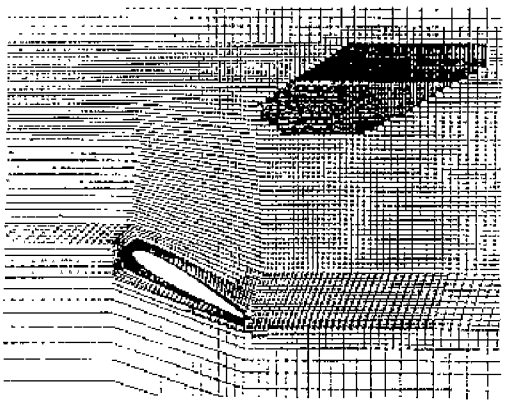

Fig. 3(a) Unstructured grid view (laminar)

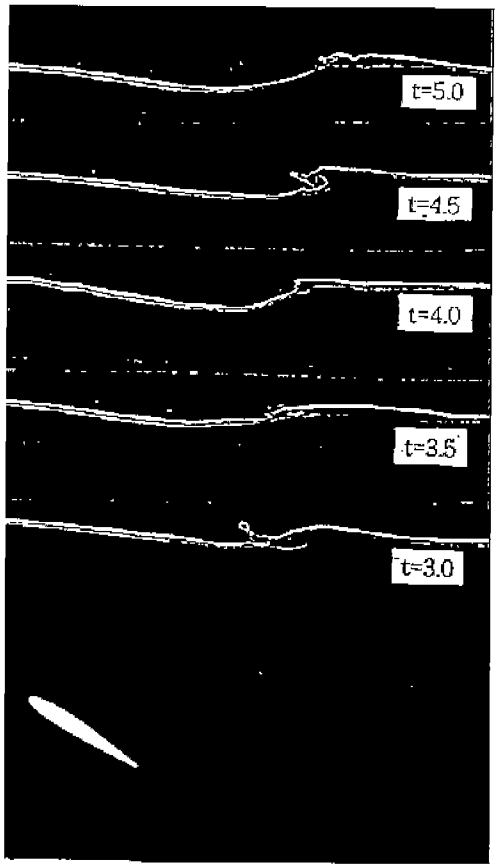

Fig. 3(b) Volume fraction(laminar)

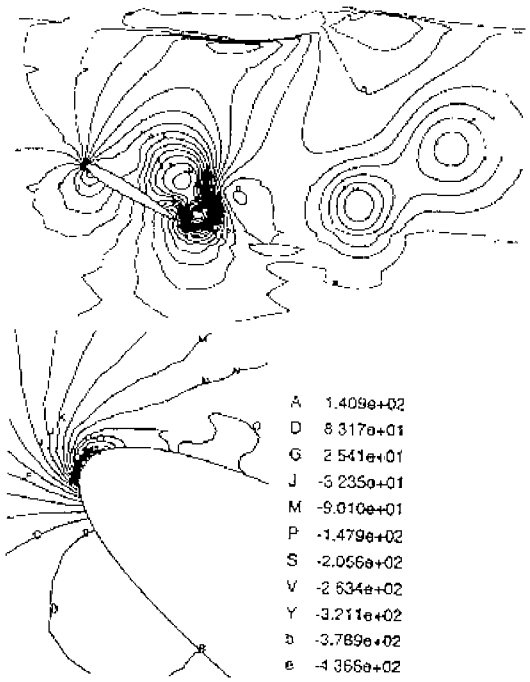

Fig. 3(c) Pressure distribution (laminar)

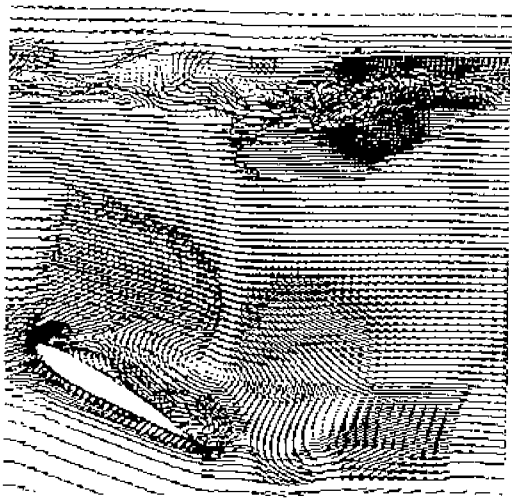

Fig. 3(d) Velocity vectors (laminar)

Fig. 2 shows the coordinate system for computation in which α is the angle of attack and d submergence depth.

Fig. 3 shows the computed results of the two fluids including free-surface for the laminar flows. Both liquid and gas flows are computed. This is important when gas is trapped in liquid or when gas flows with a high velocity. Since the grid does not have to be adapted to the shape of the free surface, problems with grid adaptations are avoided. The unstructured grid can be seen in Fig. 3(a) where the finer grid is used in some part of the free-surface and behind the trailing edge mostly influenced by the hydrofoil. The volume fraction is simulated along the time from t = 3.0 to 5.0. The breaking or overturning is well captured without any numerical difficulties. This is one of the advantages of the interface capturing method. The overall pressure contour is seen in Fig. 3(c) with a perspective view around the leading edge. The velocity vectors are simulated for two fluids: air and water region. In the computation of laminar flows, the free surface may deform in an arbitrary manner; the present interface capturing method can simulate the shape of the free surface with the surface tension.

Fig. 4 shows the computed results for the turbulent flows. As seen in Fig. 4(a), the present method predicts well the extreme deformation of the free-surface. The pressure, velocity and volume fraction are seen in Fig. 4(b), (c) and (d), respectively. In the numerical solution procedure, the outer iteration of momentum and pressure correction equations are performed first in which the value of the eddy viscosity is based on the value of k and ε at the end of the preceding iteration. After this has been completed, an outer iteration of the turbulent kinetic energy and dissipation equations is made. Since these equations are highly nonlinear, they have to be linearized prior to iteration. After completing an iteration of the turbulence model equations, it is necessary to recalculate the eddy viscosity and start a new outer iteration. Fig. 4(e) shows the contour of the kinetic energy obtained by the

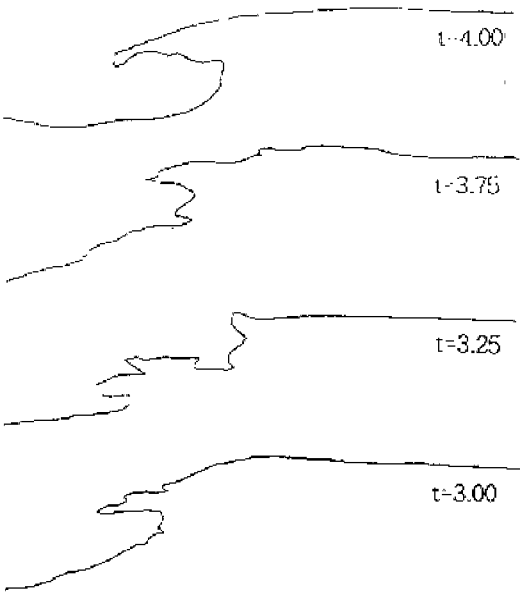

Fig. 4(a) Free surface height (turbuent)

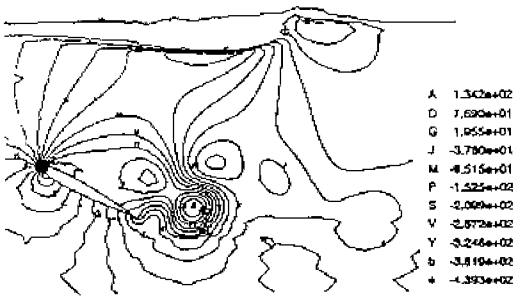

Fig. 4(b) Pressure distribution (turbulent)

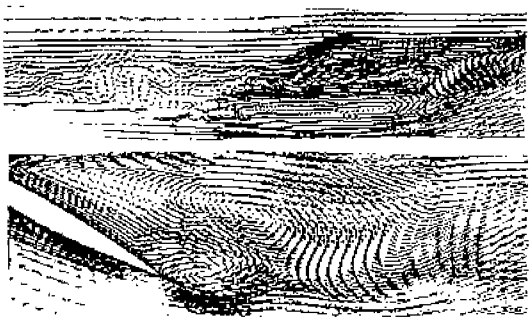

Fig. 4(c) Velocity vectors (turbulent)
(above : near free-surface)

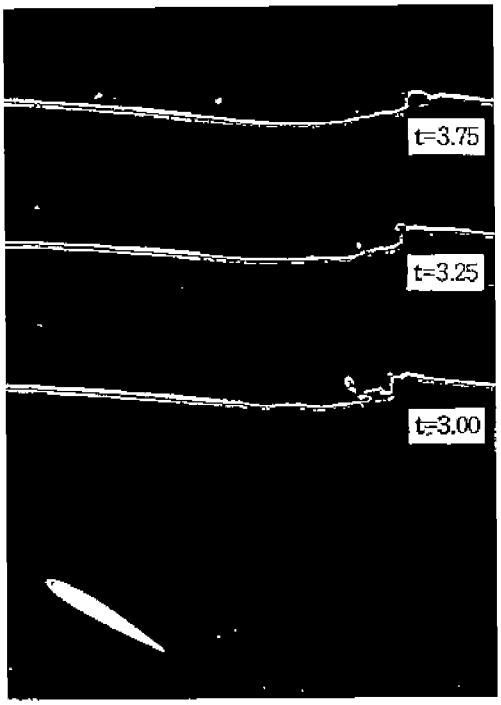

Fig. 4(d) Volume fraction (turbulent)

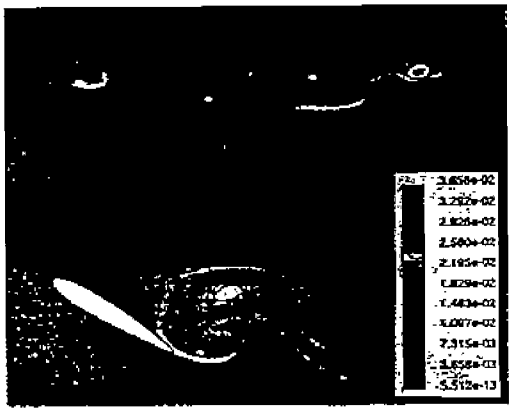

Fig. 4(e) Kinetic energy contour

turbulence model of the k-ε RNG type.

The flows around hydrofoil close to the free surface is substantially different from the flow around hydrofoil with large submergence. Computations were performed at the speed of 1.5 m/sec in deep water; in this case, a steady solution was obtained. The difference in flow patterns for the two different submergences are best illustrated by looking at the profiles of the streamwise and vertical velocity component along the lines at y= 45 mm (above hydrofoil) and y= -101 mm (below hydrofoil), from one chord length ahead to one chord length behind the foil.

For the non-breaking waves, the chord length is 203 mm, angle of attack 5° , the towing velocity 0.8 m/sec, submergence depth 210 mm, Froude number based on the foil speed and chord length is Fr= 0.567. The computations were performed using four

systematically refined grids with 1004, 4016, 16064 and 64256 CVs respectively, in order to assess the discretization errors. Fig. 5 shows the wave profiles computed on the four grids using the interface-tracking method, compared with experimental data (Duncan[3]). The difference between solutions on subsequent grids is reducing with grid refinement, indicating convergence towards a grid-independent solution. The comparison with the experimental data shows that the grid-independent numerical solution will still appreciably differ from experimental observation. For the breaking waves, a series of computations was conducted using the NACA 0012 hydrofoil with chord length of 1000 mm, submergence depth of 140 mm (measured from the mid-point on the profile nose). Fig. 6 shows the velocity vectors and free- surface shapes at four time instants for the foil speed of 1 m/sec. The hydrofoil starts suddenly moving at full speed; this leads to a build-up of a very steep, but smooth wave just above the trailing edge. This wave then overturns, as indicated in the top figure of Fig.6. After that, the breaking region moves slightly forward and remains in the range between 0.8 and 0.9 chord lengths from the nose. In the initial stage of simulation, some vortex shedding is observed; later the flow becomes smooth all around the hydrofoil. Note that the velocity scale is not the same in all figures, and that in the breaking region the velocities are very low. The dark- colored region represents volume fraction around 0.5; where the interface is sharp, this region is narrow. Large spreading of this region in the wave-breaking area indicates intensive mixing of water and air.

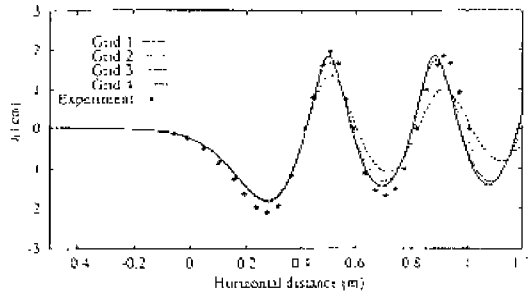

Fig. 5 Free-surface profile in the flow around a subsequent NACA0012 hydrofoil computed the interface method on the four systematically refined grids, compared to experimental data of Duncan

4. Concluding Remarks

The numerical results presented demonstrate the capabilities of interface-capturing method to compute flows around submerged hydrofoils under severe wave-breaking conditions.

Although no experimental data is available for the breaking cases, it is believed that the main features of the free-surface flows as a function of hydrofoil speed are qualitatively correctly predicted. In particular, the fact that the wave-breaking region moves towards the trailing edge and beyond as the speed increased and that the hydraulic-jump conditions are obtained above the hydrofoil appear plausible. The comparisons of numerical solutions using interface method with experimental data for the non-breaking conditions, in spite of the non-perfect agreement, suggest that the simulation results are at least qualitatively correct. Computations on the substantially finer grid are in progress and in the future also the experiments will be carried out to enable quantitative verification.

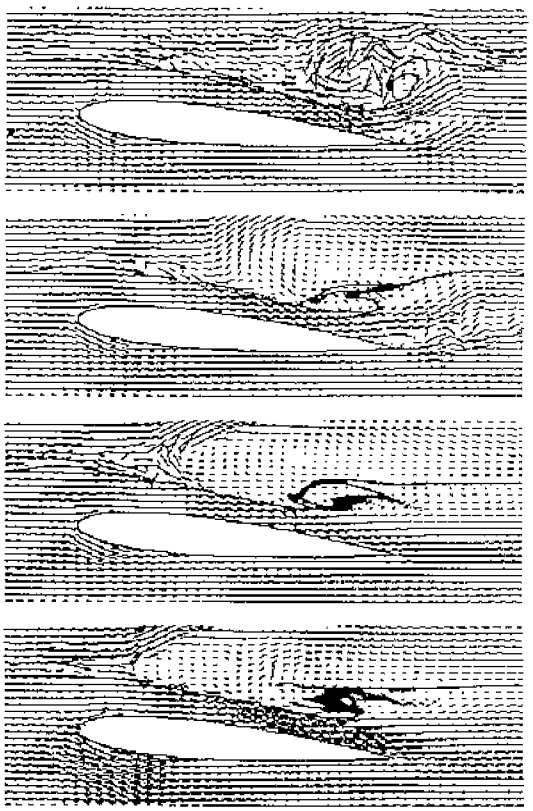

Fig. 6 Computed velocity vectors (in a coordinate frame attached to the foil) and free-surface shape at four time instants about one second apart, for the foil speed of 1.0 m/sec

References

Duncan, J. H.(1983). "The breaking and non- breaking wave resistance of a two-dimensional hydrofoil", J. Fluid Mech., Vol. 126, pp 507~520.

Farmer, J., Martinelli, L. and Jameson, A.(1994). "Fast multigrid method for solving incom- pressible hydrodynamic problems with free surfaces", AIAA J., Vol. 32, pp 1175~1182.

Leonard, B. P.(1997) "Bounded higher order upwind multi dimensional finite volume convection diffusion algolithms", in W. J. Minkowycz, E. M. Sparrow, Advances in Numerical Heat Transfer, Chap. 1, Taylor and Francis, New York, pp 1~57.

Muzaferija, S. and Peric, M.(1997). "Computation of free surface flows using finite volume method and moving grids", Numer. Heat Transfer, Part B, Vol 32, pp 369~384.

Muzaferija, S. and Peric, M.(1998). "Computation of free surface flows using interface-tracking and interface-capturing methods", Chap. 3, in O. Mahrenholtz and M. Markiewicz, Nonlinear Water Wave Interaction, Computational Mechanics Publications, Southampton.

Ubbink, O.(1997). "Numerical prediction of two fluid systems with sharp interfaces", Ph. D. Thesis, Univ of London.

1999년 11월 7일 원고 접수
2000년 2월 22일 수정본 채택